Eur. Phys. J. C (2023) 83:67
https://doi.org/10.1140/epjc/s10052-022-11162-7

THE EUROPEAN PHYSICAL JOURNAL C

Regular Article - Theoretical Physics

SMEFT deviations

Federico Camponovo[1,2,a], **Giampiero Passarino**[1,2,b]

[1] Dipartimento di Fisica Teorica, Università di Torino, Turin, Italy
[2] INFN, Sezione di Torino, Turin, Italy

Received: 1 December 2022 / Accepted: 22 December 2022 / Published online: 24 January 2023

Abstract This work is based on a bottom-up approach to the standard-model effective field theory (SMEFT), resulting in an equiprobable space of Wilson coefficients. The randomly generated Wilson coefficients of the SMEFT (in the Warsaw basis) are treated as pseudo-data and, for each observable, the corresponding probability density function is computed. The goal has been to understand how large are the deviations from the SM once the SMEFT scale (Λ) and the range of the Wilson coefficients are selected. Correlations between different observables are also discussed.

1 Introduction

The standard-model effective field theory [1] (SMEFT) is a useful tool to analyze possible deviations from the standard model (SM). In this work we will use the SMEFT (in the so-called Warsaw basis [2]) at the one- loop level. This means insertion of dim $=$ 6 operators in one-loop SM diagrams plus "pure" one loop SMEFT diagrams (i.e. diagrams with no counterpart in the SM). In particular we will study the following (pseudo-)observables:

- the g $-$ 2 of the muon, i.e. the anomalous magnetic moment a_μ,
- the value for the W boson mass, M_W, as derived by using the LEP1 input parameter set (IPS),
- the vector and axial couplings for the Z$-$ boson decay $Z \to \mu^+\mu^-$ and the corresponding $\sin^2\theta^\mu_{\rm eff}$,
- the Higgs boson decay $H \to \gamma\gamma$,
- the Higgs boson decay $H \to \bar{b}b$.

It is not the goal of this paper to describe the use and reuse of the SMEFT (for that see Ref. [3]) in fits [4–9]. The goal is instead to compute SMEFT deviations w.r.t. the SM and to understand how large they can be and the correlation among different (pseudo-) observables.

All the calculations are based on in-house codes; the analytic expressions have been obtained by using a FORM code (`SMEFTO.frm`), numerical results by using a FORTRAN code (`SMEFTO.f`). General definitions and notations can be found in Refs. [10,11], examples of observables in Ref. [3]. The strategy of the calculation will be as follows. Given an observable $\mathscr{O}$ we first compute $\mathscr{O}^{(4)}$, i.e. $\mathscr{O}$ at dimension four (the SM). If $M_{\mathscr{O}}$ is the corresponding matrix element then

$$\mathscr{O}^{(4)} = \int \mathrm{dPS} \sum_{\rm spin} |\, M^{(4)}_{\mathscr{O}}\,|^2, \tag{1}$$

where dPS indicates the corresponding phase-space integration. Including SMEFT (i.e. dimension six operators) we will have

$$M_{\mathscr{O}} = M^{(4)}_{\mathscr{O}} + \frac{g_6}{\sqrt{2}} M^{(6)}_{\mathscr{O}}, \qquad g_6 = \frac{1}{G_F\,\Lambda^2}, \tag{2}$$

giving the full $\mathscr{O}^{(6)}$. Note that both dim $=$ 4 and dim $=$ 6 terms may or may not contain loop corrections. Here we have introduced $g_6^{-1} = G_F\,\Lambda^2$, where G_F is the Fermi coupling constant and Λ is the SMEFT scale. Two options will follow, linear or quadratic SMEFT. In the first case only the linear term will be kept in squaring the amplitude.

After having computed the relevant quantities we will define deviations

$$\Delta\,\mathscr{O} = \mathscr{O}^{(6)}/\mathscr{O}^{(4)} - 1, \tag{3}$$

and ① plot the relative probability density function (pdf) by randomly generating the corresponding set of Wilson coefficients, ② display relationships between observables.

Quoting [12] we can say that *good scientific research can be characterised by a fruitful interaction between fundamental theories, phenomenological models and effective field theories. All of them have their appropriate functions in the*

[a] e-mail: federico.camponovo@unito.it
[b] e-mail: giampiero@to.infn.it (corresponding author)

research process. Therefore, we identify our "conservative" scenario and will not deal with "matching-motivated" strategies; it is clear that the model space does not necessarily project evenly on all SMEFT parameters but our approach will be purely bottom-up. To summarize:

- In a top-down approach we are assuming a space of UV-complete models $M_i(\{p_M\})$ functions of their parameters (masses and couplings). By UV-completion we mean passing from the SM to a more general quantum field theory (QFT) above a threshold; the more general QFT should explain more experimental data than the SM. We are not addressing here the question posed by Georgi [13]: *it may even be possible that there is no end and, simply more and more scales as one goes to higher and higher energies*. From the space $\mathscr{M}$ we ideally derive the corresponding low-energy limit, taking into account those models that can be described by the SMEFT; these limits and mixings of heavy Higgs bosons are discussed in Ref. [11] heavy-light contributions in Ref. [14]. In the low-energy limit we obtain a space of Wilson coefficients $\mathscr{W}(\{a\})$; each parameter of $\mathscr{M}$ is now translated into a set of Wilson coefficients. Of course there will be limitations on $\mathscr{M}$, e.g. models M_i should respect custodial symmetry [15].
- In a purely bottom-up approach [12] (our framework), $\mathscr{W}$ defines our computable "theory", see Ref. [16]. Our "conservative" scenario is realized by generating values for the Wilson coefficients with the random number generator `RANLUX` [17]. In the bottom-up approach "equiprobable" is a a prior in the sense that we assume zero knowledge of the UV (except for the possible option of suppressing operators containing field strengths) so we assume that any Wilson coefficient is as likely as any other.

In order to arrive at the final result we will have to (briefly) discuss the main ingredients of the calculation.

2 SM and SMEFT renormalization

We will not discuss renormalization of the SMEFT in great details. To summarize what has been done (for full details see Refs. [10,11,18]) we will define a renormalization procedure.

- After the specification of the gauge fixing term including the corresponding ghost Lagrangian we select a renormalization scheme and a choice of the IPS. Every counterterm for the parameters in the Lagrangian contains an arbitrary UV-finite constant. Any explicit definition of the constant is a definition of the renormalization scheme.
- It will be enough to say that the SMEFT, as any QFT, depends on parameters and on fields. Our strategy is to define counterterms (CT) for the parameters, to introduce an IPS and to perform on-shell renormalization for the SM parameters and the $\overline{\rm MS}$ renormalization for the Wilson coefficients, see Appendix A. Beyond two-point functions this will require a mixing of the Wilson coefficients.

Some comment is needed on external leg wave-function factors: external unstable particles represent a notorious problem, see Refs. [19,20]. Here we will follow the strategy developed for LEP observables. As a consequence the wave function factors are taken to be real; of course, one should introduce the notion of complex poles but the Z-observables (and also the H-observables) have not been described in terms of complex poles.

Removal of UV-poles is not the end of any renormalization procedure, see Ref. [21]. For instance, after removing the UV-poles, we need to connect the renormalized $SU(2)$ coupling constant (g_R) to the fine structure constant $\alpha(0)$ or to the Fermi coupling constant G_F. Most of the renormalization procedure has to do with two-point functions, therefore we recall few definitions

$$S_{\gamma\gamma} = \frac{g^2 s_\theta^2}{16\pi^2}\,\Pi_{\gamma\gamma}(p^2)\,p^2, \qquad S_{Z\gamma} = \frac{g^2 s_\theta}{16\pi^2 c_\theta}\,\Sigma_{Z\gamma}(p^2),$$
$$S_{ZZ} = \frac{g^2}{16\pi^2 c_\theta^2}\,\Sigma_{ZZ}(p^2), \qquad S_{WW} = \frac{g^2}{16\pi^2}\,\Sigma_{WW}(p^2), \tag{4}$$

where s_θ is the (bare) sine of the weak-mixing angle. The procedure is as follows:

① Introduce the transition $S_{Z\gamma}$ and the corresponding self-energy $S_{\gamma\gamma}$.
② Define the $\gamma\bar{1}1$ vertex at LO (but including SMEFT terms) and compute the corresponding amplitude for Coulomb scattering obtaining

$$\mathscr{A}^c_{LO} = \Gamma_{LO}\,\gamma^\mu \otimes \gamma_\mu. \tag{5}$$

③ Introduce the Dyson resummed γ propagator and define (residue of the pole at zero momentum transfer)

$$\mathscr{A}(g_R) = \Gamma^2_{LO}\left[1 - \Pi_{\gamma\gamma}\,|_{p^2=0}\right]^{-1}. \tag{6}$$

④ Introduce CTs for g and mix the Wilson coefficients. It will follow that the dimension four is UV-finite after introducing the parameter CTs and dimension six is UV-finite after mixing.

⑤ Next we write the equations

$$\mathscr{A}(g_R) = 4\,\pi\,\alpha(0), \quad g_R^2 = \frac{4\pi\,\alpha(0)}{s_\theta^2}\left\{1 + \frac{g_6}{\sqrt{2}}\,\delta g_0^{(6)} + \frac{\alpha(0)}{\pi}\left[\delta g^{(4)} + \frac{g_6}{\sqrt{2}}\,\delta g_1^{(6)}\right]\right\}, \tag{7}$$

where g_6 id defined in Eq. (2), and fix the δ g (UV-finite) CTs, i.e. the δg in Eq. (7) are the unknowns to be fixed by solving the (UV-finite) renormalization equations.

Of course, this procedure requires the well-known WST identities for the cancellation of vertices and wave function factors at $p^2 = 0$. What we have here is that this WST identity is, well known for QED, proven for the SM [21,22], proven to be valid in the SMEFT by our explicit calculations.

Of course we also need the relation between g_R and the Fermi coupling constant. The derivation follows in a similar way.

3 Computing (pseudo-)observables

We have selected the IPS containing M_W and M_Z. The first observable to be considered is the g − 2 of the muon. After computing the (QED) Schwinger term we have included the one-loop SM contributions and added the dimension six contributions. The strategy is, as described, to make UV-renormalization, to separate the IR/collinear QED corrections, and to develop an efficient algorithm for computing the $p^2 \to 0$ limit. For a model-independent analysis of the magnetic and electric dipole moments of the muon and electron see Ref. [23].

As far as $Z \to \mu^+\mu^-$ is concerned we will adopt the LEP strategy, see Refs. [24,25]: the explicit formulae for the $Z\bar{1}1$ vertex are always written starting from a Born-like form of a pre-factor times a fermionic current, where the Born parameters are promoted to effective, scale-dependent parameters

$$\gamma^\mu\left(\mathscr{G}_V^f + \mathscr{G}_A^f\,\gamma^5\right). \tag{8}$$

The corresponding width (LEP1 conventions) is

$$\Gamma(Z \to \bar{1}1) = 4\,\Gamma_0\left[|\,\mathscr{G}_V^f\,|^2\ R_V^1 + |\,\mathscr{G}_A^f\,|^2\ R_A^1\right], \qquad \Gamma_0 = \frac{G_F\,M_Z^3}{24\sqrt{2}\,\pi}, \tag{9}$$

where the radiator factors describe the final state QED and QCD corrections and take into account the fermion mass. Next define $g_{V,A}^f$ as the real part of $\mathscr{G}_{V,A}^f$ and define

$$\sin^2\theta_{\rm eff}^\mu = \frac{1}{4}\left(1 - \frac{g_V^\mu}{g_A^\mu}\right). \tag{10}$$

The processes $H \to \gamma\gamma$ and $H \to \bar{b}b$ do not need additional comments.

Predicting the W mass means changing the IPS. Therefore we start from the following equations:

$$\frac{1}{g^2 s_\theta^2} = \frac{1}{4\pi\,\alpha} + \frac{1}{16\,\pi^2}\,\Pi_{\gamma\gamma}(0),$$
$$8\,\frac{M^2}{g^2} = \frac{\sqrt{2}}{G_F} + \frac{1}{16\,\pi^2}\left[\Sigma_{WW}(0) + M^2\,s_\theta^2\,\delta_G\right],$$
$$\frac{M^2}{c_\theta^2} = M_Z^2 + \frac{g^2}{16\,\pi^2\,c_\theta^2}\,\Re\,\Sigma_{ZZ}(M_Z^2), \tag{11}$$

where g, s_θ and M are bare parameters and Π and Σ are self-energies containing dimension six contributions. In the second equation δ_G collects the contributions to the muon decay coming from vertices and boxes. While $\delta_G^{4)}$ has been known since a long time [26] we still miss a complete calculation of $\delta_G^{(6)}$. This missing ingredient should be considered as contributing to the SMEFT "theoretical uncertainty".

By solving the set of renormalization equations we obtain bare parameters as a function of experimental data. It is always convenient to resum large logarithmic corrections so that the lowest-order resummed solution for the weak-mixing angle will be

$$s_\theta^2 = \bar{s}^2 = \frac{1}{2}\left\{1 - \left[1 - 4\,\frac{\pi\,\alpha(M_Z^2)}{\sqrt{2}\,G_F\,M_Z^2}\right]^{1/2}\right\}. \tag{12}$$

By s_θ we mean the Lagrangian parameter while will reserve the notation θ_W for $\sin^2\theta_W = 1 - M_W^2/M_Z^2$. Inserting the solutions into the inverse W propagator returns M_W with a lowest-order solution given by $M_W = \bar{c}\,M_Z$ which receives corrections in perturbation theory, including the ones due to dimension six operators.

It is worth noting that the inclusion of dimension six operators touches all the ingredients of the calculation. For instance we have

$$\alpha(M_Z) = \alpha(0)\left[1 - \Delta\alpha_l - \Delta\alpha_t - \Delta\alpha_{\rm had}^{(5)}\right]^{-1} \tag{13}$$

Corrections due to leptons and to the top quark contain both dim = 4 and dim = 6 terms; the hadronic part is taken, as usual from data.

It is important to understand that the inclusion of dim = 6 only in tree-diagrams introduces blind directions in the space of Wilson coefficients. The inclusion of loops partially removes the degeneracy.

4 Numerical results

For the masses we use the values quoted by the PDG and define two scenarios corresponding to

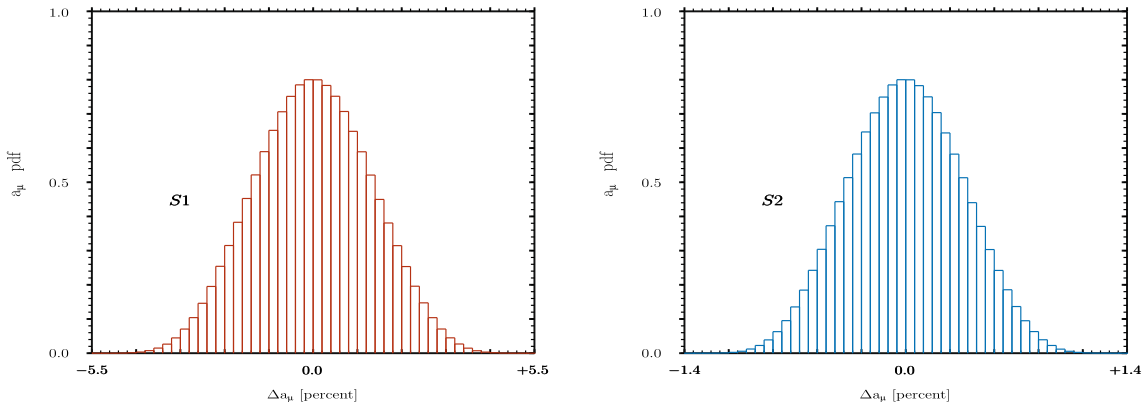

Fig. 1 The pdf for Δa_μ. Left figure refers to scenario S1, right figure to scenario S2

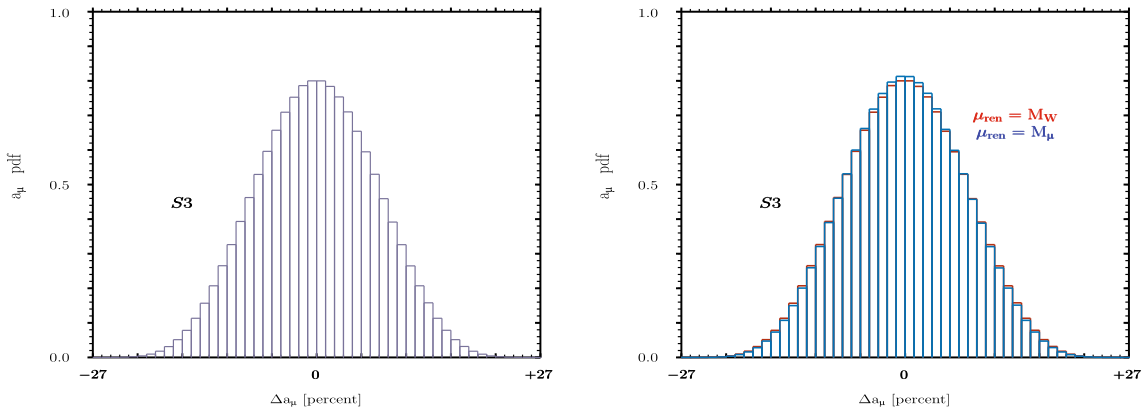

Fig. 2 The pdf for Δa_μ. $\Lambda = 1$ Tev and Wilson coefficients $\in [-0.5, +0.5]$

S1 $\Lambda = 1$ Tev with values of the (renormalized) Wilson coefficients $\in [-0.1, +0.1]$.
S2 $\Lambda = 2$ Tev with values of the (renormalized) Wilson coefficients $\in [-0.1, +0.1]$.

We start with the observation that $\alpha(M_Z)$ in the SMEFT differs from the SM value by less than a permille.

4.1 SMEFT and a_μ

The accepted theoretical value for a_μ is 0.00116591810 (43) [27]; the new experimental world-average results today is 0.00116592061 (41) [28] with a difference of 251×10^{-11}. Given the one-loop EW contribution [29]

$$a_\mu^{EW}\ |_{\text{one-loop}} = \frac{G_F\, M_\mu^2}{24\sqrt{2}\,\pi^2}\left[5 + \left(1 - 4\,\sin^2\theta_W\right)^2\right] \quad (14)$$

where $\sin^2_W = 0.22301$, we obtain $a_\mu^{EW} = 194.8 \times 10^{-11}$ at one loop (higher order EW corrections bring this value to 153.6×10^{-11} [30]). Therefore the new experimental value requires deviations of $\mathcal{O}(100)$ percent w.r.t. the SM which are obviously difficult to reach in the context of the SMEFT. For instance, with $\Lambda = 1$ Tev and Wilson coefficients $\in [-0.5, +0.5]$ we can reach a 50% deviations but only in the corners of the space of Wilson coefficients. Note that at tree level a_μ depends only on a_{1W} and a_{1B} (Wilson coefficients in the Warsaw basis).

We define

$$\Delta a_\mu = \frac{a_\mu^{(6)}}{a_\mu^{(4)}} - 1, \qquad a_\mu^{(4)} = a_\mu^{EW}\ |_{\text{oneloop}}\ . \quad (15)$$

In Fig. 1 we show the pdf for Δa_μ. Left figure refers to S1, right figure to S2. We have also produced results for $\Lambda = 1$ Tev and Wilson coefficients $\in [-0.5, +0.5]$. The result is shown in Fig. 2.

We have also investigated a scenario where $\Lambda = 1$ Tev, Wilson coefficients $\in [-1, +1]$ and where we discard points in the space of Wilson coefficients where $|\ \Delta \sin^2\theta^\mu_{\text{eff}}\ | > 10^{-3}$. In the resulting distribution the largest fraction of Δa_μ deviations is compatible with zero. From the histograms we derive an approximate value for the standard deviation of the pdf: they are $\sigma = 0.357$ for S2, $\sigma = 1.428$ for S1 and $\sigma = 7.142$ for the last scenario (Fig. 3). For the sake of completeness we have repeated the calculation assuming the all Wilson coefficients are positive; the result shows a mean $\mu = 1.414$ with $\sigma = 1.429$

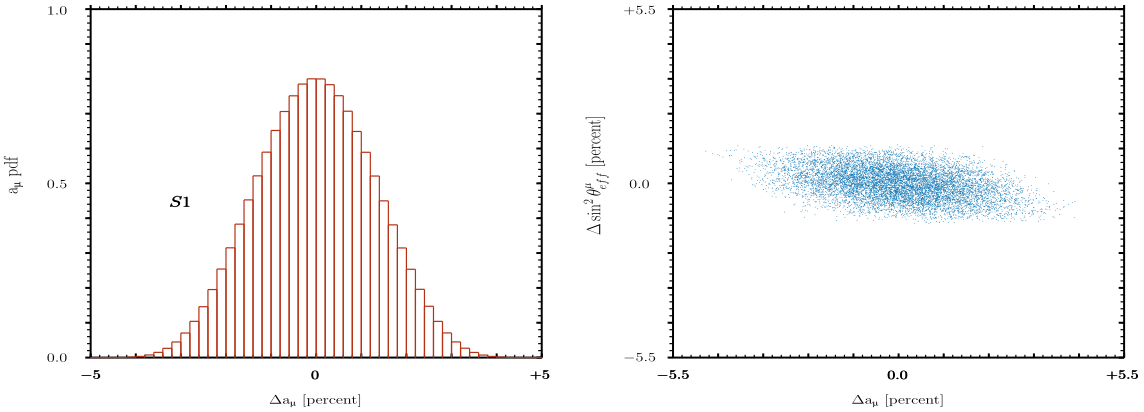

Fig. 3 The pdf for $\Delta \sin^2\theta^{\mu}_{\rm eff}$ in scenario S1 (left figure). A scattered plot displaying the relationship between Δa_μ and $\Delta \sin^2\theta^{\mu}_{\rm eff}$ (right figure)

By looking at the data we can ask "what happens when we put constraints on the space of Wilson coefficients"? The situation seems to be the following: there is one combination of Wilson coefficients (in the Warsaw basis), $a_{l\,WB} = \sin\theta_W\, a_{l\,W} - \cos\theta_W\, a_{l\,B}$, which appears at tree level in the calculation of a_μ but only at one-loop in the other pseudo-observables. Selecting large values for $a_{l\,WB}$ while putting to zero the remaining Wilson coefficients could do the job. It is worth noting that according to Ref. [31] $a_{l\,WB}$ is the Wilson coefficient of a Loop-Generated operator (containing field strengths), thus requiring a loop suppression factor. The relevance of $a_{l\,W}$, $a_{l\,B}$ (called $a_{e\,W,B}$ in Ref. [2]) becomes clear when we observe that the corresponding operators contain $\sigma^{\mu\nu}$.

To give an example, suppose that we use the SMEFT at the tree level; let us define

$$a_{\phi\,l\,V} = a^{(3)}_{\phi\,l} - a^{(1)}_{\phi\,l} - a_{\phi\,l}, \quad a_{\phi\,l\,A} = a^{(3)}_{\phi\,l} - a^{(1)}_{\phi\,l} + a_{\phi\,l}, \tag{16}$$

where the a are Wilson coefficients in the Warsaw basis. We can derive both of them in terms of other Wilson coefficients by asking zero deviation in the vector and axial couplings of the Z− boson. Then we fix $a_{l\,WB} = \sin\theta_W\, a_{l\,W} - \cos\theta_W\, a_{l\,B}$ in order to reproduce the a_μ deviation with the rest of the Wilson coefficients left free. Always accepting to work at tree level, if we fix the free Wilson coefficients $\in [-0.1, +0.1]$ values of $a_{l\,WB}/(16\pi^2) > 0.01$ are needed to reach 50% deviations for a_μ.

Alternatively, we can proceed as follows: every observable can be decomposed as

$$\mathcal{O} = \mathcal{O}^{(4)} + \frac{g_6}{\sqrt{2}}\left[\delta^{(6)}_{\mathcal{O}} + \frac{G_F\, M_W^2}{\pi^2}\,\Delta^{(6)}_{\mathcal{O}}\right]. \tag{17}$$

The first term in Eq. (17) represents the tree-level contribution in the SMEFT while the second accounts for loops in SMEFT. We have set to zero the $\delta^{(6)}$ terms in the vector and axial couplings of the Z boson, which means two linear conditions among Wilson coefficients.

The resulting scattered plot is shown in Fig. 4. The interesting fact in comparing the left and right figures is that the tree-level SMEFT correction is dominant but the one-loop SMEFT contribution is not negligible [32,33]. In the right panel of Fig. 2 we have shown the (tiny) effect of changing the renormalization scale.

For $\Lambda = 1$ Tev and Wilson coefficients $\in [-0.1, +0.1]$, although we have reduced the deviations for $\sin^2\theta^{\mu}_{\rm eff}$ at the level of $\pm 0.2\%$ we can only obtain deviations for a_μ at the level of $\pm 4\%$ (Fig. 5).

4.2 SMEFT and $Z \to \mu^+\mu^-$

LEP data [24] return $\sin^2\theta^{l}_{\rm eff} = 0.23153 \pm 0.00016$ (the error is 0.07 %). The natural comment is that it is extremely difficult to evade this bound. Despite this evidence we should observe the following facts: the LEP1 data were used to predict $M_W = 80.363 \pm 0.032$ GeV (we use 80.379 GeV) and the Higgs boson mass was not an input parameter, it was obtained $M_H < 285$ GeV at 95 % C.L.

The pdf for $\sin^2\theta^{\mu}_{\rm eff}$ is shown in Fig. 3 for S1 and where we have defined

$$\Delta \sin^2\theta^{\mu}_{\rm eff} = \frac{\sin^2\theta^{\mu}_{\rm eff}\;|_{\rm dim=6}}{\sin^2\theta^{\mu}_{\rm eff}\;|_{\rm dim=4}} - 1. \tag{18}$$

We should remember that the corresponding experimental error is 0.07%. From the histogram we derive the following approximate deviation, $\sigma = 0.498$.

- From the scattered plot of Fig. 3 we observe that, due to the low correlation, it is still possible to accommodate large deviations for a_μ while keeping (very) low deviations for $\sin^2\theta^{\mu}_{\rm eff}$.

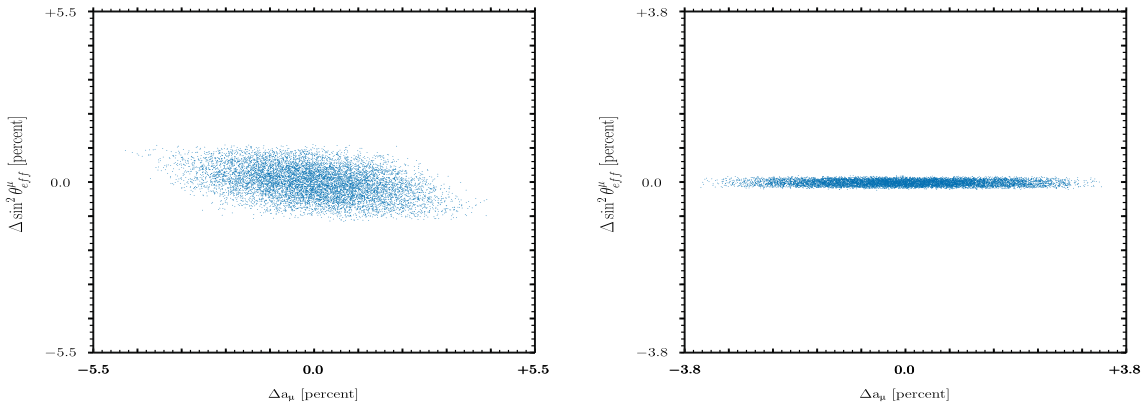

Fig. 4 A scattered plot displaying the relationship between Δa_μ and $\Delta \sin^2\theta^\mu_{\rm eff}$. Left figure is the same as in Fig. 3. Right figure takes into account the constraint described in Eq. (17)

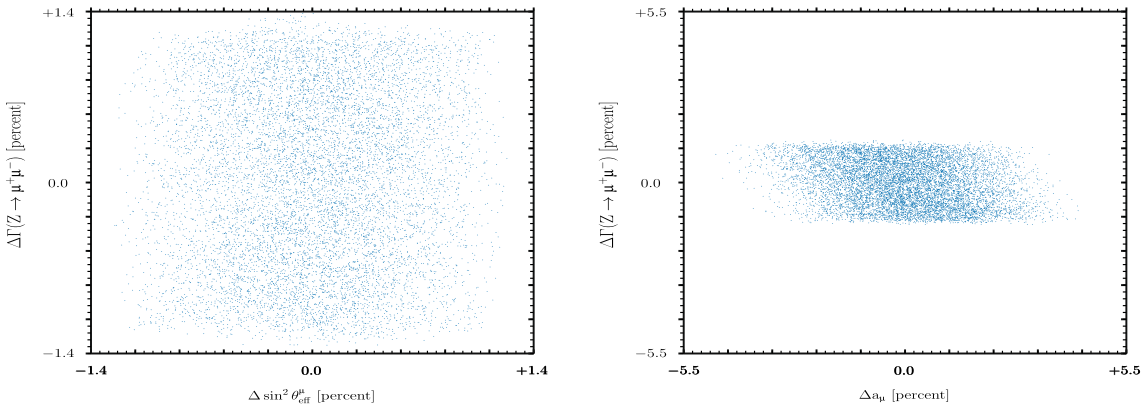

Fig. 5 A scattered plot displaying the relationship between $\Delta(Z \to \mu^+\mu^-)$ and $\Delta \sin^2\theta^\mu_{\rm eff}$ (left figure) or Δa_μ (right figure)

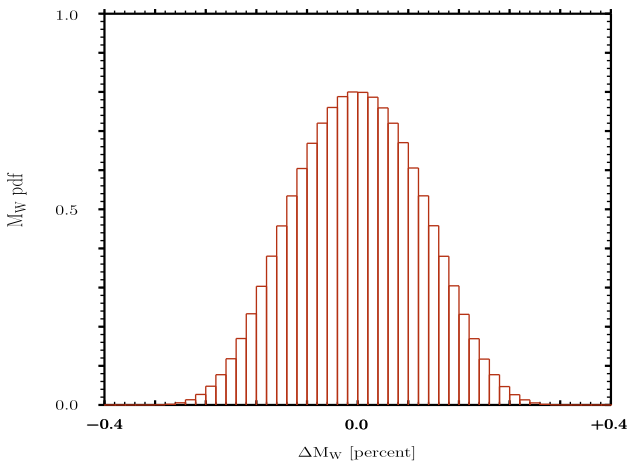

Fig. 6 The pdf for ΔM_W, scenario S1

4.3 SMEFT and M_W

The result from the CDF II detector is $M_W = 80.4335 \pm 0.0094\,\text{GeV}$ [34] to be compared with the previous world-average, $M_W = 80.379 \pm 0.012\,\text{GeV}$ [35]. Therefore we require a deviation of $+0.068\%$. For fits see Ref. [36]. Our result for the ΔM_W pdf are shown in Fig. 6. From the histogram we derive the following approximate deviation, $\sigma = 0.098$.

4.4 SMEFT and $H \to \gamma\gamma$, $H \to \bar{b}b$

In Fig. 7 we show a scattered plot displaying the relationship between the set of "data" corresponding to $Z \to \mu^+\mu^-$ and $H \to \gamma\gamma$.

In Fig. 7 we show a scattered plot displaying the relationship between the set of "data" corresponding to $Z \to \mu^+\mu^-$ and $H \to \bar{b}b$. For $H \to \bar{b}b$ we use the deconvoluted result (both QED and QCD).

From LHC Run 1 Higgs results (combined ATLAS and CMS results as reported in Ref. [5]) the $\gamma\gamma$ decay (production mechanism ggH) the signal strength is $1.10^{+0.23}_{-0.22}$ while the $\bar{b}b$ decay (VH production) is 1.0 ± 0.5 (1.01 ± 0.20 for Run 2).

4.5 Impact of QED corrections on $Z \to \mu^+\mu^-$

Let us consider QED corrections to the decay $Z \to \mu^+\mu^-$. After adding up virtual and real contributions and defining

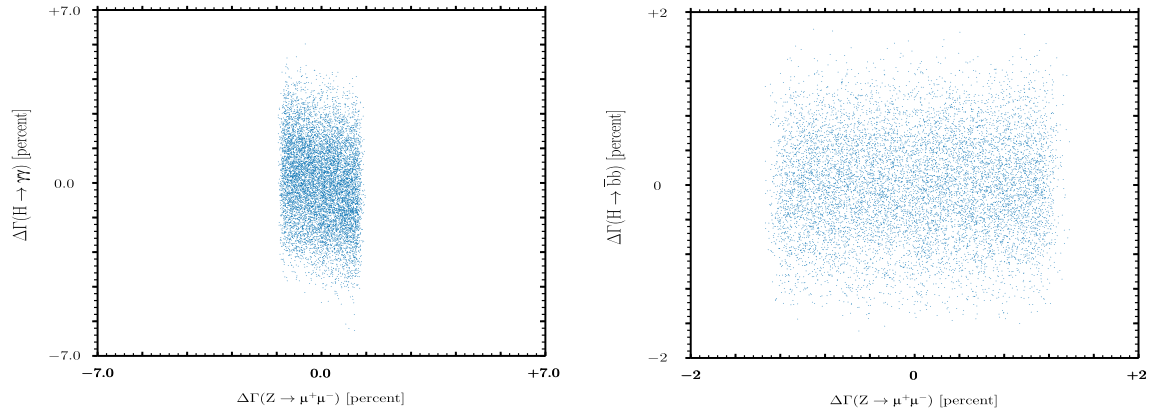

Fig. 7 A scattered plot displaying the relationship between $\Delta\Gamma(Z \to \mu^+\mu^-)$ and $\Delta\Gamma(H \to \gamma\gamma)$ (left figure) or $\Delta\Gamma(H \to \bar{b}b)$ (right figure)

the linear combination of Wilson coefficients, the final result for the decay width is an IR/collinear-free quantity, both in the SM and in the SMEFT. The result can be written as

$$\Gamma_{QED}(Z \to \mu^+\mu^-) = \frac{3}{4}\frac{\alpha}{\pi}\Gamma_0 \times \left[(1+v_1^2)\left(1+\frac{g_6}{\sqrt{2}}\delta_1^{(6)}\right)+\frac{g_6}{\sqrt{2}}\delta_2^{(6)}\right], \quad (19)$$

with $v_1 = 1-4\ \sin^2\theta_W$, showing a double (SM and SMEFT) factorization. The explicit expressions for the $\delta^{(6)}$ terms can be found in Ref. [37]. The scattered plot displaying the relationship between $\Delta\sin^2\theta^{\mu}_{\text{eff}}$ and $\Delta\Gamma_{QED}(Z \to \mu^+\mu^-)$ is shown in Fig. 8.

This result is important, not only for extending IR/collinear finiteness to the SMEFT but also because it shows that higher dimensional operators enter everywhere: signal, background and radiation. The latter is particularly relevant when one wants to include (SM-deconvoluted) EW precision observable constraints in a fit to Higgs data. Since LEP POs are (mostly) SM- deconvoluted, the effect of dim = 6 operators on the deconvolution procedure should be checked carefully.

In Eq. (19) Γ_0 is the LO width and the LEP definition is

$$\Gamma^{\text{dec}}(Z \to \bar{l}1) = \frac{\Gamma(Z \to \bar{l}1)}{1+\frac{3}{4}\frac{\alpha(M_Z^2)}{\pi}}. \quad (20)$$

Once again, fitting the deconvoluted pseudo-observable as reported at LEP with the SMEFT is not fully consistent.

5 Conclusions

Without looking at the experimental data we have assumed a bottom-up approach described by the SMEFT. Therefore, the randomly generated Wilson coefficients of the SMEFT (in the Warsaw basis) are treated as pseudo-data and, for each observable, we have computed the corresponding probability density function.

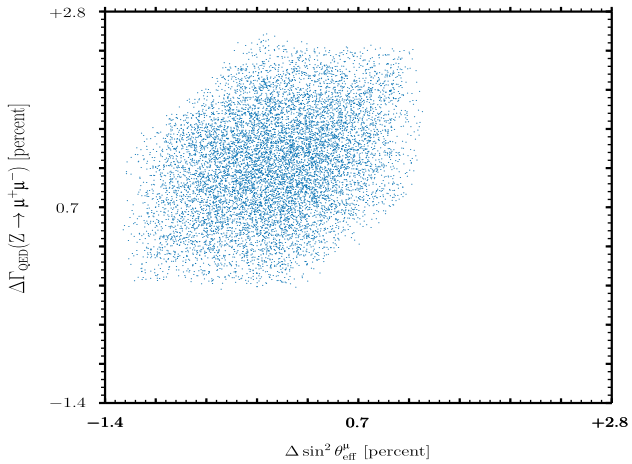

Fig. 8 A scattered plot displaying the relationship between $\Delta\Gamma_{QED}(Z \to \mu^+\mu^-)$ and $\Delta\sin^2\theta^{\mu}_{\text{eff}}$

The equiprobability bias (EB) is a tendency to believe that every process in which randomness is involved corresponds to a fair distribution, with equal probabilities for any possible outcome. It has been shown that the EB is actually not the result of a conceptual error about the definition of randomness. On the contrary, the mathematical theory of randomness does imply uniformity [38].

Stated differently we consider a single "supersystem" where we identify the values of the Wilson coefficients and implement the principle that equal ignorance should be represented by equiprobability.

Our goal has been to understand how large are the deviations from the SM once the SMEFT scale (Λ) and the range of the Wilson coefficients are selected. Theory-driven research [39] focuses on identifying abstract constructs and the relationships among them.

Our set of pseudo-observables includes a_μ, $\sin^2\theta^{\mu}_{\text{eff}}$, M_W, $\Gamma(Z \to \mu^+\mu^-)$, $\Gamma(H \to \gamma\gamma)$ and $\Gamma(H \to \bar{b}b)$. The corresponding results can be compared with the experimental data to understand how easy or difficult will be to explain (possi-

ble) SM-deviations in terms of the SMEFT language. In particular, constraints in the space of Wilson coefficients have been introduced to explain large deviations for one observable and very small deviations for a second observable. These constraints put you on the hedge of the equiprobable space of Wilson coefficients with some of them taking "very" large values.

Theories can be changed by data or even invalidated by them. We have an initial theory (the SM) and a theory of deviations (the SMEFT), and then we add and absorb new data, altering the theories at each point.

Acknowledgements G. P. gratefully acknowledges a constructive correspondence with A. David.

Data Availability Statement This manuscript has no associated data or the data will not be deposited. [Authors' comment: Data sharing not applicable to this article as no datasets were generated or analysed during the current study.]

Funded by SCOAP[3]. SCOAP[3] supports the goals of the International Year of Basic Sciences for Sustainable Development.

Appendix A: Details on renormalization

Since a large part of the renormalization procedure depends on two-point functions we briefly summarize the procedure. Let X be any boson field, the inverse X propagator (with $p^2 = -s$) is

$$-\mathrm{s} + \mathrm{m}_\mathrm{X}^2 - \frac{\mathrm{g}^2}{16\pi^2}\,\Sigma_\mathrm{X}(\mathrm{s}), \tag{A.1}$$

where m_X is the bare X mass. We introduce CTs, i.e.

$$\mathrm{m}_\mathrm{X} = \mathrm{m}_\mathrm{X}^{\mathrm{ren}}\left\{1 + \frac{\mathrm{g}^2}{16\pi^2}\left[\delta^{(4)}_{\mathrm{m}_\mathrm{X}} + \frac{\mathrm{g}_6}{\sqrt{2}}\,\delta^{(6)}_{\mathrm{m}_\mathrm{X}}\right]\right\}, \tag{A.2}$$

and remove s−independent UV poles. Next we write the renormalization equation at $\mathrm{s} = \mathrm{M}_\mathrm{X}^2$ where M_X is the physical (on-shell) mass.

$$\Sigma_\mathrm{X}(\mathrm{s}) = \Sigma_\mathrm{X}(\mathrm{M}_\mathrm{X}^2) + (\mathrm{s} - \mathrm{M}_\mathrm{X}^2)\,\Sigma'_\mathrm{X}(\mathrm{m}_\mathrm{X}^2) + \mathrm{rest}. \tag{A.3}$$

Introducing now

$$\mathrm{m}_\mathrm{X}^{\mathrm{ren}} = \mathrm{M}_\mathrm{X}\left\{1 + \frac{\mathrm{g}^2}{16\pi^2}\left[\Delta^{(4)}_{\mathrm{m}_\mathrm{X}} + \frac{\mathrm{g}_6}{\sqrt{2}}\,\Delta^{(6)}_{\mathrm{m}_\mathrm{X}}\right]\right\}, \tag{A.4}$$

we fix the new CTS such that

$$\mathrm{M}_\mathrm{X}^2 = \mathrm{m}_\mathrm{X}^2 - \frac{\mathrm{g}^2}{16\pi^2}\,\Re\,\Sigma_\mathrm{X}(\mathrm{M}_\mathrm{X}^2), \tag{A.5}$$

and derive the corresponding wave-function factors. For fermions the procedure requires the introduction of $1 \pm \gamma^5$ projectors and will not be repeated here.

The inclusion of vertices and boxes in the amplitude (after the introduction of the wave-function factors for the external legs) is such that

- for the SM (dim = 4) the amplitudes are UV finite,
- for the SMEFT (dim = 6) we have to introduce a mixing

$$\begin{aligned} \mathrm{a}_i &= \mathrm{Z}_{ij}\,\mathrm{a}_j^{\mathrm{ren}}, \\ \mathrm{Z}_{ij} &= \delta_{ij} + \frac{\mathrm{g}^2}{16\pi^2}\left[\delta\mathrm{Z}^{(4)}_{ij} + \frac{\mathrm{g}_6}{\sqrt{2}}\,\delta\mathrm{Z}^{(6)}_{ij}\right], \end{aligned} \tag{A.6}$$

where a_i are Wilson coefficients.

References

1. A.V. Manohar, Introduction to effective field theories, in: *Les Houches Summer School: EFT in Particle Physics and Cosmology Les Houches*, Chamonix Valley, July 3–28, 2017 (2018). arXiv:1804.05863
2. B. Grzadkowski, M. Iskrzynski, M. Misiak, J. Rosiek, Dimension-six terms in the standard model Lagrangian. JHEP **10**, 085 (2010). https://doi.org/10.1007/JHEP10(2010)085. arXiv:1008.4884
3. A. David, G. Passarino, Use and reuse of SMEFT. arXiv:2009.00127
4. I. Brivio, Y. Jiang, M. Trott, The SMEFTsim package, theory and tools. JHEP **12**, 070 (2017). https://doi.org/10.1007/JHEP12(2017)070. arXiv:1709.06492
5. J. Ellis, C.W. Murphy, V. Sanz, T. You, Updated global SMEFT fit to Higgs, diboson and electroweak data. JHEP **06**, 146 (2018). https://doi.org/10.1007/JHEP06(2018)146. arXiv:1803.03252
6. C.W. Murphy, Statistical approach to Higgs boson couplings in the standard model effective field theory. Phys. Rev. D **97**(1), 015007 (2018). https://doi.org/10.1103/PhysRevD.97.015007. arXiv:1710.02008
7. J. Ellis, M. Madigan, K. Mimasu, V. Sanz, T. You, Top, Higgs, diboson and electroweak fit to the standard model effective field theory. JHEP **04**, 279 (2021). https://doi.org/10.1007/JHEP04(2021)279. arXiv:2012.02779
8. J.J. Ethier, G. Magni, F. Maltoni, L. Mantani, E.R. Nocera, J. Rojo, E. Slade, E. Vryonidou, C. Zhang, Combined SMEFT interpretation of Higgs, diboson, and top quark data from the LHC. JHEP **11**, 089 (2021). https://doi.org/10.1007/JHEP11(2021)089. arXiv:2105.00006
9. N. Castro, K. Cranmer, A.V. Gritsan, J. Howarth, G. Magni, K. Mimasu, J. Rojo, J. Roskes, E. Vryonidou, T. You, LHC EFT WG Report: Experimental measurements and observables (2022). https://doi.org/10.48550/ARXIV.2211.08353. arXiv:2211.08353

10. M. Ghezzi, R. Gomez-Ambrosio, G. Passarino, S. Uccirati, NLO Higgs effective field theory and κ-framework. JHEP **07**, 175 (2015). https://doi.org/10.1007/JHEP07(2015)175. arXiv:1505.03706
11. G. Passarino, XEFT, the challenging path up the hill: dim = 6 and dim = 8. arXiv:1901.04177
12. S. Hartmann, Effective field theories, reductionism and scientific explanation. Stud. Hist. Philos. Mod. Phys. **32**, 267–304 (2001). https://doi.org/10.1016/S1355-2198(01)00005-3
13. H. Georgi, Effective field theory. Annu. Rev. Nucl. Part. Sci. **43**, 209–252 (1993). https://doi.org/10.1146/annurev.ns.43.120193.001233
14. F. del Aguila, J. de Blas, M. Perez-Victoria, Electroweak limits on general new vector bosons. JHEP **09**, 033 (2010). https://doi.org/10.1007/JHEP09(2010)033. arXiv:1005.3998
15. I. Low, J. Lykken, G. Shaughnessy, Have we observed the Higgs (imposter)? Phys. Rev. D **86**, 093012 (2012). https://doi.org/10.1103/PhysRevD.86.093012. arXiv:1207.1093
16. G. Passarino, Veltman, renormalizability, calculability. Acta Phys. Polon. B **52**(6–7), 533 (2021). https://doi.org/10.5506/APhysPolB.52.533. arXiv:2104.13569
17. F. James, RANLUX: a FORTRAN implementation of the high quality pseudorandom number generator of Luscher. Comput. Phys. Commun. **79**, 111–114 (1994) [Erratum: Comput. Phys. Commun. 97, 357 (1996)]. https://doi.org/10.1016/0010-4655(94)90233-X
18. K. Costello, *Renormalization and Effective Field Theory, Mathematical Surveys and Monographs*, vol. 170 (American Mathematical Society, Providence, 2011)
19. S. Actis, G. Passarino, Two-loop renormalization in the standard model part II: renormalization procedures and computational techniques. Nucl. Phys. B **777**, 35–99 (2007). https://doi.org/10.1016/j.nuclphysb.2007.03.043. arXiv:hep-ph/0612123
20. S. Actis, G. Passarino, Two-loop renormalization in the standard model part III: renormalization equations and their solutions. Nucl. Phys. B **777**, 100–156 (2007). https://doi.org/10.1016/j.nuclphysb.2007.04.027. arXiv:hep-ph/0612124
21. D.Y. Bardin, G. Passarino, The standard model in the making: precision study of the electroweak interactions (1999)
22. S. Dittmaier, All-order renormalization of electric charge in the Standard Model and beyond, in: *15th International Symposium on Radiative Corrections: Applications of Quantum Field Theory to Phenomenology AND LoopFest XIX: Workshop on Radiative Corrections for the LHC and Future Colliders* (2021). arXiv:2109.03528
23. J. Aebischer, W. Dekens, E.E. Jenkins, A.V. Manohar, D. Sengupta, P. Stoffer, Effective field theory interpretation of lepton magnetic and electric dipole moments. JHEP **07**, 107 (2021). https://doi.org/10.1007/JHEP07(2021)107. arXiv:2102.08954
24. The ALEPH, DELPHI, L3, OPAL, SLD Collaborations, the LEP Electroweak Working Group, the SLD Electroweak and Heavy Flavour Groups, Precision electroweak measurements on the Z resonance. Phys. Rep. **427**, 257 (2006). arXiv:hep-ex/0509008
25. D.Y. Bardin, M. Grunewald, G. Passarino, Precision calculation project report. arXiv:hep-ph/9902452
26. W.F.L. Hollik, Radiative corrections in the standard model and their role for precision tests of the electroweak theory. Fortsch. Phys. **38**, 165–260 (1990). https://doi.org/10.1002/prop.2190380302
27. The anomalous magnetic moment of the muon in the standard model. Phys. Rep. **887**, 1–166 (2020). https://doi.org/10.1016/j.physrep.2020.07.006
28. G.W. Bennett et al., Final report of the muon E821 anomalous magnetic moment measurement at BNL. Phys. Rev. D **73**, 072003 (2006). https://doi.org/10.1103/PhysRevD.73.072003. arXiv:hep-ex/0602035
29. W.A. Bardeen, R. Gastmans, B.E. Lautrup, Static quantities in Weinberg's model of weak and electromagnetic interactions. Nucl. Phys. B **46**, 319–331 (1972). https://doi.org/10.1016/0550-3213(72)90218-0
30. A. Czarnecki, W.J. Marciano, A. Vainshtein, Refinements in electroweak contributions to the muon anomalous magnetic moment. Phys. Rev. D **67**, 073006 (2003) [Erratum: Phys. Rev. D 73, 119901 (2006)]. https://doi.org/10.1103/PhysRevD.67.073006. arXiv:hep-ph/0212229
31. M.B. Einhorn, J. Wudka, The bases of effective field theories. Nucl. Phys. B **876**, 556–574 (2013). https://doi.org/10.1016/j.nuclphysb.2013.08.023. arXiv:1307.0478
32. G. Passarino, M. Trott, The standard model effective field theory and next to leading order. arXiv:1610.08356
33. A. Freitas, D. López-Val, T. Plehn, When matching matters: loop effects in Higgs effective theory. Phys. Rev. D **94**(9), 095007 (2016). https://doi.org/10.1103/PhysRevD.94.095007. arXiv:1607.08251
34. T. Aaltonen et al., High-precision measurement of the W boson mass with the CDF II detector. Science **376**(6589), 170–176 (2022). https://doi.org/10.1126/science.abk1781
35. R.L. Workman et al., Review of particle physics. PTEP **2022**, 083C01 (2022). https://doi.org/10.1093/ptep/ptac097
36. E. Bagnaschi, J. Ellis, M. Madigan, K. Mimasu, V. Sanz, T. You, SMEFT analysis of M_W. JHEP **08**, 308 (2022). https://doi.org/10.1007/JHEP08(2022)308. arXiv:2204.05260
37. M. Boggia et al., The HiggsTools handbook: a beginners guide to decoding the Higgs sector. J. Phys. G **45**(6), 065004 (2018). https://doi.org/10.1088/1361-6471/aab812. arXiv:1711.09875
38. N. Gauvrit, K. Morsanyi, The equiprobability bias from a mathematical and psychological perspective. Adv. Cogn. Psychol. **10**, 119–130 (2014). https://doi.org/10.5709/acp-0163-9
39. W. Maas, J. Parson, S. Purao, V. Storey, C. Woo, Data-driven meets theory-driven research in the era of big data: opportunities and challenges for information systems research. J. Assoc. Inf. Syst. **19**, 1253–1273 (2018). https://doi.org/10.17705/1jais.00526